

Running head:

**Auxin Efflux and Cytoskeletal Arrangement in BY-2 Cells**

Corresponding author:

**Eva Zažímalová,**

**Institute of Experimental Botany, The Academy of Sciences of the Czech Republic,**

**Rozvojová 135, CZ-16502 Prague 6, Czech Republic**

**telephone: +420-2-20390-429**

**fax: +420-2-20390-474**

**e-mail: [eva.zazim@ueb.cas.cz](mailto:eva.zazim@ueb.cas.cz)**

Journal area:

**Development and Hormone Action**

Title:

**Differential Effects of 1-N-Naphthylphthalamic Acid and Brefeldin A on the Cytoskeleton and Endoplasmic Reticulum During the Inhibition of Auxin Efflux from BY-2 Tobacco Cells**

Authors:

Jan Petrášek, Adriana Černá, Kateřina Schwarzerová, Miroslav Elčknér, David Arthur Morris<sup>2</sup> and Eva Zažímalová\*

Addresses:

Institute of Experimental Botany, The Academy of Sciences of the Czech Republic, Rozvojová 135, CZ-16502 Prague 6, Czech Republic (J.P., M.E., D.A.M., E.Z.); and Department of Plant Physiology, Faculty of Science, Charles University, Viničná 5, CZ-128 44 Prague 2, Czech Republic (J.P., A.Č., K.S.)

Footnotes:

<sup>1</sup> This work was supported by the EU, INCO Copernicus (grant no. ERBIC15 CT98 0118 to E.Z.), by the Ministry of Education, Youth and Sports of the Czech Republic (project no. LN00A081), and by the UK Royal Society and the Academy of Sciences of the Czech Republic under the European Science Exchange Scheme (grant to D.A.M.).

<sup>2</sup> Present address: Division of Cell Sciences, School of Biological Sciences, University of Southampton, Bassett Crescent East, Southampton SO16 7PX, UK

\* Corresponding author; e-mail [eva.zazim@ueb.cas.cz](mailto:eva.zazim@ueb.cas.cz), fax +420-2-20390-474

Abstract:

To investigate the role of the cytoskeleton in the mechanism and regulation of auxin transport, the effects of the potent auxin transport inhibitor 1-*N*-naphthylphthalamic acid (NPA) and the vesicle-trafficking inhibitor brefeldin A (BFA) on both auxin accumulation and cytoskeleton arrangement were studied in suspension-cultured interphase cells of BY-2 tobacco (*Nicotiana tabacum* L., cv. Bright Yellow) cell line. Both NPA and BFA treatments rapidly increased auxin (naphthalene-1-acetic acid) accumulation by the cells in a concentration-dependent manner, but their effects on the arrangement of the cytoskeleton differed. BFA caused a rearrangement of radial and perinuclear actin filaments into clusters, and a gradual disintegration of the endoplasmic reticulum. Microtubules were unaffected by BFA treatment. NPA had no effect on any of these structures. Taken together, these results emphasize the importance of radial and perinuclear, but not cortical, actin filaments in vesicle-mediated trafficking of component(s) of the auxin efflux carrier system. The results are discussed with respect to the suggestion that cycling of the auxin efflux catalyst between the plasma membrane and endomembranes is actin-dependent and responds differentially to BFA and NPA.

## Introduction

The polar transport of auxins (such as indole-3-acetic acid, IAA) plays a crucial role in the regulation of growth and development in plants (Davies, 1995). A large body of experimental evidence supports the proposal by Rubery and Sheldrake (1974) and Raven (1975) that auxin transport polarity results from the differential permeabilities of each end of transporting cells to auxin anions ( $\text{IAA}^-$ ) and protonated auxin molecules ( $\text{IAAH}$ ; reviewed by Goldsmith, 1977). Undissociated  $\text{IAAH}$  (a weak organic acid) is relatively lipophilic and can readily enter cells by diffusion from the more acidic extracellular space; the  $\text{IAA}^-$  anion, on the other hand, is hydrophilic and does not cross membranes easily. Consequently, auxins tend to accumulate in plant cells by a process of “anion trapping” and exit the symplast with the intervention of transmembrane auxin anion efflux carriers (Goldsmith, 1977). There is now overwhelming evidence that the differential efflux of  $\text{IAA}^-$  anions from the two ends of auxin-transporting cells results from an asymmetric (polar) distribution of such carriers (see Goldsmith, 1977; Lomax et al., 1995). Genes encoding putative auxin influx and efflux carriers have been identified from *Arabidopsis* and other species (reviewed recently by Morris, 2000; Muday and DeLong, 2001; Friml and Palme, 2002); and it has been shown that efflux (and possibly influx) carrier proteins are targeted to specific regions of the plasma membrane (PM) in auxin transporting cells (e.g. see Gälweiler et al., 1998; Müller et al., 1998; Swarup et al., 2001; reviewed by Friml and Palme, 2002).

Studies employing specific inhibitors of components of the polar auxin transport process have played a major role in shaping our understanding of the polar auxin transport machinery. The most widely used inhibitor of auxin efflux is 1-*N*-naphthylphthalamic acid (NPA), a well-characterized member of a group of inhibitors

known as phytoalexins (Rubery, 1990). The application of NPA to various plant tissues results in the inhibition of auxin efflux carrier activity and consequently increases auxin accumulation in cells (reviewed by Morris, 2000). Although the mechanism of its inhibitory action on polar transport remains obscure, it is believed to be mediated by a specific, high affinity, NPA-binding protein (NBP; Sussman et al., 1980; Rubery, 1990). This has been shown to be a peripheral membrane protein located on the cytoplasmic face of the PM and associated with the cytoskeleton in zucchini (*Cucurbita pepo* L.) hypocotyl cells (Cox and Muday, 1994; Dixon et al., 1996; Butler et al., 1998; but cf. Bernasconi et al., 1996). Protein synthesis inhibitors such as cycloheximide (CH) rapidly uncouple carrier-mediated auxin efflux and the inhibition of efflux by NPA (Morris et al., 1991). In the short term, however, CH has no effect on either the specific and saturable NPA binding or on auxin efflux itself, leading to the suggestion that the NBP and the efflux catalyst may interact through a third, rapidly turned over protein (Morris et al., 1991; discussed in Morris, 2000).

Inhibitors of Golgi-mediated vesicle traffic, such as brefeldin A (BFA) and monensin, also very rapidly inhibit auxin efflux carrier activity in zucchini hypocotyl tissue (Wilkinson and Morris, 1994; Morris and Robinson, 1998), and suspension-cultured tobacco cells (Delbarre et al., 1998). They also inhibit polar auxin transport through tissue (Robinson et al., 1999). However, the time lag for inhibition of efflux-carrier activity by BFA (minutes) is considerably shorter than the lag for inhibition of efflux activity by protein synthesis inhibitors (up to 2 hours; Morris et al., 1991). This implies that efflux catalysts turn over very rapidly in the PM without a requirement for concurrent protein synthesis, a situation that contrasts sharply with the inhibitory action of NPA on auxin efflux which does require concurrent protein synthesis (see above). Results of a detailed comparison of the effects of CH and BFA on efflux

carrier activity revealed that efflux carrier proteins probably cycle between the PM and an unidentified intracellular compartment (Robinson et al., 1999; cf. Delbarre et al., 1998), a possibility strongly supported by the observation that *AtPIN1*, a member of a family of putative *Arabidopsis* auxin efflux carrier proteins (see Friml and Palme, 2002), is rapidly and reversibly internalized following BFA treatment of *Arabidopsis* roots (Geldner et al., 2001).

It has been suggested recently that polar auxin transport inhibitors might also reduce auxin efflux by blocking actin-dependent efflux carrier protein cycling and vesicle trafficking as part of a general and non-specific effect on protein traffic (Geldner et al., 2001). Treatment of *Arabidopsis* roots with the polar auxin transport inhibitor 2,3,5-triiodobenzoic acid (TIBA) prevented the BFA-induced internalization of *AtPIN1* and prevented the traffic of internalized *PIN1* to the PM after BFA washout (Geldner et al., 2001). This would have the effect of reducing the density of carriers in the PM available for auxin efflux. Similar effects of TIBA on a rapidly turned over PM-ATPase and the *KNOLLE* gene product (a syntaxin involved in vesicle docking – see Muday and Murphy, 2002) were observed, suggesting a rather general action of TIBA on Golgi-mediated protein traffic to the PM (Geldner et al., 2001).

The site-directed traffic of auxin efflux carrier proteins involves not only the Golgi mediated secretory system itself, but also the participation of components of the cytoskeletal system. The application of cytochalasin (an actin-depolymerizing agent) reduced polar auxin transport in corn coleoptiles (Cande et al., 1973) and in zucchini hypocotyls (Butler et al., 1998). Moreover, cytochalasin D has been shown recently to block cycling of the

putative auxin efflux carrier protein, PIN1, between endosomal compartments and the plasma membrane in *Arabidopsis* roots (Geldner et al., 2001). These observations are consistent with an important role for actin filaments (AFs) in the proper localization and function of components of the auxin efflux carrier complex (reviewed by Muday 2000; Muday and Murphy 2002). Evidence from a careful *in vitro* biochemical analysis of the association between the NBP and the cytoskeleton in membrane preparations from zucchini hypocotyls, indicates a strong link between NPA action and the actin cytoskeleton (Butler et al 1998). Only treatments that stabilised F-actin (phalloidin) but not those that stabilized microtubules (taxol) increased NPA-binding activity. Furthermore, direct interaction between the high-affinity NPA binding protein and F-actin was proven by F-actin affinity chromatography in the same system (Hu et al 2000).

Despite the observations discussed above which link the inhibition of efflux carrier activity by NPA to effects of NPA on actin-dependent and Golgi vesicle-mediated targeting of efflux carrier protein to the plasma membrane, almost nothing is known about the effects (if any) of NPA or other phytohormones on the organization of components of the cytoskeleton or the vesicle secretion system. Given the possibility that phytohormones might have a general effect on vesicle traffic to the PM and on cycling of proteins between the PM and endosomal compartments (as suggested by Geldner et al 2001), some physical disruption of the secretory pathway and/or cytoskeleton might be expected to occur following the application of these compounds. However, to the best of our knowledge, no such disruption has so far been reported.

Here, we report an investigation to compare the action of BFA and NPA on both auxin accumulation and the arrangement and structure of components of the secretory pathway and the cytoskeleton (viz. AFs, microtubules, MTs, and endoplasmic reticulum, ER) in suspension-cultured BY-2 tobacco cells. Using a new quantitative method to study the rearrangement of AFs and the formation of actin clusters in the perinuclear region of cells, we show that whilst both of these compounds increase auxin accumulation by inhibiting auxin efflux, only BFA has an effect on the structure of AFs and of the ER. Our observations lead us to suggest that whilst radial and perinuclear (but possibly not cortical) AFs and ER are required for normal auxin efflux, the inhibitory action of NPA on efflux does not involve any changes in cytoskeleton and ER.

## **RESULTS**

### **Effects of NPA and BFA on the Accumulation of Auxin**

The rate of [<sup>3</sup>H]-labeled naphthalene-1-acetic acid ([<sup>3</sup>H]NAA) accumulation by BY-2 cells is shown in Fig. 1 (A and B). After an initial period of rapid uptake lasting 3 to 10 min depending on experiment, uptake settled to a slower, steady rate that was maintained for up to 40 min. Accumulation was extremely sensitive to NPA and was stimulated approximately threefold in the presence of 10 μM or 50 μM NPA (Fig. 1A). An NPA concentration dependence study indicated that [<sup>3</sup>H]NAA accumulation was maximally stimulated by as little as 1.0 μM NPA and that the stimulatory effect of NPA began to decline rapidly at concentrations around or greater than 100 μM (Fig. 2A). Because of the greatly reduced stimulation of [<sup>3</sup>H]NAA accumulation at high concentrations of NPA, possibly caused by toxic side effects not directly related

to auxin efflux, the maximum concentration of NPA employed in subsequent cytological observations was restricted to 50  $\mu$ M.

A similar picture emerged in the case of BFA (Fig. 1B, 2B), although the maximum stimulation of [ $^3$ H]NAA accumulation (at between 10  $\mu$ M and 40  $\mu$ M BFA) was lower than that caused by NPA (cf. Fig. 1, A and B, and 2, A and B). As with NPA, high concentrations of BFA (100  $\mu$ M) reduced the stimulation of [ $^3$ H]NAA accumulation (Fig. 1B, 2B).

Over the uptake period used here, no significant metabolism of [ $^3$ H]NAA by cells of BY-2 was detected. Apart from a small amount of label that remained at the origin in all chromatography solvents used (less than 10 % of the total label recovered), the recovered ethanol-soluble radioactivity migrated as a single spot which had the same mobility on cellulose thin layer plates as authentic [ $^3$ H]NAA (data not shown).

### **Effects of BFA and NPA on the Arrangement of Actin Filaments and Microtubules**

To test the reaction of the cytoskeleton to the application of agents that modify polar auxin transport, the arrangement of both AFs and MTs in BFA- and NPA-treated cells was studied during a 30-min incubation period in parallel with the auxin accumulation measurements described above. Since the cell populations used to measure auxin accumulation were predominantly in interphase, we investigated the arrangement of the interphase cytoskeleton (MTs and AFs in the cortical cytoplasm and AFs in the transvacuolar strands and perinuclear region). Typical interphase BY-2 tobacco cells contained fine and transversally oriented AFs (Fig. 3A) and MTs (Fig. 3G) in the cortical cytoplasm, together with radially oriented AFs in transvacuolar strands and in

perinuclear region (Fig. 3D). There were no MTs in transvacuolar strands and around the nucleus in interphase cells (Fig. 3G). Although both NPA and BFA significantly increased auxin accumulation to roughly the same extent (Fig. 1, 2), their effects on cytoskeleton arrangement differed considerably. Whilst the fine cortical AFs and MTs retained their transverse orientation after 30-min treatment with 20  $\mu$ M BFA (Fig. 3, B and H), BFA had a dramatic effect on the arrangement of the radial and perinuclear AFs (Fig. 3E). Fine AFs in the transvacuolar strands collapsed and actin became concentrated in clusters around the nucleus (Fig. 3E).

We have developed a new procedure for the evaluation of quantitative changes in actin aggregation in the perinuclear region utilizing image analysis software (refer to Material and Methods, and Fig 4). This procedure was used to evaluate the effects of BFA and it was shown that the degree of actin aggregation noticeably increased with duration of treatment (Fig. 4E). The highest BFA concentration tested (100  $\mu$ M) was shown to be inhibitory for actin aggregation in the same way that it was inhibitory for auxin accumulation (cf. Figs 4E and 2B). The effect of BFA on AFs was reversible and 30 min after wash out of BFA with fresh medium, the actin clusters disappeared and the density variation (DV) parameter decreased again to control values (Fig. 4F).

In contrast to BFA, 30-min incubation in 50  $\mu$ M NPA did not cause any changes in the arrangement of AFs in cortical region (Fig. 3C; cf. Fig 3, A and B) as well as around the nucleus and in the transvacuolar strands (Fig. 3F; cf. Fig. 3, D and E). Correspondingly, cortical MTs were also unaffected after 30 min in 50  $\mu$ M NPA (Fig. 3I; cf. Fig. 3, G and H).

## **The Effect of BFA and NPA on the Arrangement of Endoplasmic Reticulum**

In addition to the Golgi apparatus, the plant endoplasmic reticulum has also been shown to be sensitive to BFA treatment (Henderson et al., 1994). Therefore we investigated if the ER was also affected in cells in which BFA or NPA stimulated the accumulation of auxin. The behavior of endoplasmic reticulum in interphase cells of BY-2 after NPA or BFA treatment was followed *in vivo* using cells transformed with the pBIN m-*gfp5*-ER plant binary vector coding for the ER-localized fusion protein (mGFP5-ER). In exponentially growing control interphase cells, ER was present in the form of a tubular network penetrating not only the cortical layer of cytoplasm (Fig. 5A), but also the transvacuolar strands and perinuclear region (Fig. 5D). Within this network, small motile bodies were observed (video sequence can be seen at [http://www.ueb.cas.cz/laboratory\\_of\\_hormonal\\_regulations/BFAmovies.htm](http://www.ueb.cas.cz/laboratory_of_hormonal_regulations/BFAmovies.htm)). The movement of these bodies was observed over the surface of the network of ER tubules that constantly changed its orientation and pattern. Treatment of cells with 20  $\mu$ M BFA for 30 min resulted in disintegration of the fine tubular network of ER, the formation of large sheets of ER, and the aggregation of the signal into a large number of bright fluorescence spots (Fig. 5B). Video sequence can be seen at [http://www.ueb.cas.cz/laboratory\\_of\\_hormonal\\_regulations/BFAmovies.htm](http://www.ueb.cas.cz/laboratory_of_hormonal_regulations/BFAmovies.htm). However, the first observable effects of BFA were clear after only 5 min (data not shown), when disintegration of the tubular network and formation of fluorescent spots started. On the other hand, even after 30 min of 20  $\mu$ M BFA treatment there were still cells with no obvious damage of ER. The accumulation of GFP fluorescence was also observed in the perinuclear region (Fig. 5E). Moreover, the movement of small motile bodies inside ER tubules decreased during a 30-min incubation in 20  $\mu$ M BFA and had almost stopped by the end of that time period. Longer treatment with 20  $\mu$ M BFA

(7 hours) resulted in the formation of large sheets of ER and intensively fluorescing bodies of irregular shape and size (data not shown).

In contrast to BFA, a 30-min incubation in 50  $\mu$ M NPA had no observable effects on either ER structure or arrangement (Fig. 5, C and F); furthermore, no changes in the movement of small bodies were found.

## DISCUSSION

### **Auxin Accumulation by BY-2 Cells is Stimulated by Both NPA and BFA**

Previous studies with suspension-cultured tobacco cells (cv. Xanthi XHFD8) have demonstrated that NAA accumulation is controlled predominantly by the activity of the auxin efflux carrier (Delbarre et al., 1996). Uptake studies presented in this paper confirmed that the accumulation of [ $^3$ H]NAA by suspension-cultured BY-2 tobacco cells was stimulated by treatment with NPA and BFA, and in a concentration-dependent manner (Fig. 1 and 2). A surprising feature of the results was that the stimulation of [ $^3$ H]NAA accumulation was saturated by as little as  $10^{-6}$  M NPA (Fig. 2A; half-saturation approx.  $10^{-7}$  M). This concentration is rather lower than that required to saturate [ $^3$ H]NAA accumulation in the VBI-0 tobacco cell line (Petrášek et al. 2002; saturation around  $10^{-5}$  M; half-saturation approx.  $10^{-6}$  M) and one that is dramatically lower than the concentration of  $2 \times 10^{-4}$  M mentioned by Geldner et al. (2001) to be necessary to perturb the cycling of PIN1 protein in *Arabidopsis* roots in the presence of BFA. The concentration of TIBA, NPA or other auxin transport (efflux) inhibitor required to perturb the cycling of PIN1 in the absence of BFA is not known; despite their obvious relevance, the effects of such treatments were not reported by Geldner et al. (2001). Thus the stimulation of [ $^3$ H]NAA accumulation (inhibition of efflux) by NPA in tobacco cells observed here and elsewhere (Delbarre

et al., 1996; Petrášek et al., 2002) is unlikely to have been caused by perturbation of efflux carrier cycling. Indeed, in the present study, concentrations of NPA exceeding about  $10^{-5}$  M caused a substantial, concentration-dependent decrease in NAA accumulation (Fig. 2A; cf. Fig. 1A). Although in the VBI-0 tobacco cell line no decrease of accumulation was observed at concentrations of NPA as high as  $10^{-4}$  M, concentrations of NPA exceeding  $10^{-5}$  M caused abnormalities in cell division and loss of cell polarity (Petrášek et al. 2002). Thus concentrations of NPA which greatly exceed the concentration necessary to saturate efflux inhibition may cause damaging effects to cells unrelated to the ability of NPA to block auxin efflux. Interestingly, although BFA itself also strongly promoted [ $^3$ H]NAA accumulation, in the cell suspensions used in our experiments the maximum stimulation observed (at  $10^{-5}$  M BFA: Fig. 1B, 2B; 22.7 % at 20 min) was substantially less than the maximum caused by NPA treatment (Fig. 1A, 2A; 130.2% at 20 min). Similar to NPA, at high concentrations of BFA (above  $3 \times 10^{-5}$  M), the stimulation of auxin accumulation was greatly reduced (Fig. 1B, 2B).

### **Actin Filaments but Not Microtubules Are Affected by BFA**

Although a role for the cytoskeleton in the polar transport of auxin has been established (for review see Muday, 2000), few microscopic data are available on the state of AFs and MTs after disruption of polar auxin transport with inhibitors. In the present study, we investigated the effects of NPA and BFA on the arrangement and structure of the cytoskeleton in suspension cultured cells of BY-2 tobacco at the same stage of development (2-day old suspensions containing predominantly interphase cells) as those used to study the effects of NPA and BFA on [ $^3$ H]NAA accumulation (see above). Staining components of the cytoskeleton with fluorescent dyes revealed

that in untreated (control) cell of this type AFs and MTs are arranged in a transverse orientation in the cortical layers of cytoplasm (Fig. 3, A and G); only AFs, but not MTs, were present in the perinuclear region and transvacuolar strands (Fig. 3D). These observations agree with those from earlier studies on BY-2 (for review see Kumagai and Hasezawa, 2001).

The arrangement of MTs and AFs in the cortical cytoplasm was not affected by 30-min treatment with BFA (20, 40 and 100  $\mu\text{M}$ ; results shown in Fig. 3, B and H, are for 20  $\mu\text{M}$ ). This is in agreement with data published by Saint-Jore et al. (2002) who reported that treatment of BY-2 cells with 180  $\mu\text{M}$  BFA for 5 h did not affect cortical MTs and AFs. However, we found that in the perinuclear region, BFA (20  $\mu\text{M}$ ) caused actin to aggregate into clusters (Fig. 3E). To the best of our knowledge this is the first report of this phenomenon from plants, although a limited number of investigations on animal cells have shown that BFA causes disruption of both AFs and MTs in normal rat kidney cells after extended treatment periods (Alvarez and Sztul, 1999). The lack of information about perinuclear actin possibly stems from the fact that most studies have concentrated on AFs in cortical layer of cytoplasm, and the perinuclear region has largely been overlooked (cf. Satiat-Jeunemaitre et al., 1996; Saint Jore et al., 2002). Recently, Waller et al. (2002) reported an increased membrane association of cortical actin after BFA treatment and bundling of cortical AFs in maize epidermal cells. This suggests that even cortical actin can be modified by treatment with BFA. Since phalloidin (used here for actin cytoskeleton visualization) binds preferentially to F-actin, it is likely that the newly formed actin clusters produced in the perinuclear region consist of the filamentous form of actin. A possible explanation for the formation of the perinuclear actin clusters is that actin may play a role in the process of ER-Golgi apparatus fusion after BFA treatment (cf.

Ritzenthaler et al., 2002). This possibility requires further testing using *in vivo* approaches with fluorescent proteins.

Image analysis was used for the quantification of the effect of BFA concentration on the formation of actin clusters in perinuclear region (Fig. 4). The method measures the “coherency” of the fluorescent signal in the perinuclear region, the less coherent the signal, the greater the extent of actin aggregation. After 30-min treatment, aggregation was greatest at 40  $\mu$ M BFA, but substantially lower at the highest concentration of BFA tested (100  $\mu$ M; Fig. 4E). A possible interpretation is that at such high concentrations of BFA, the ER-Golgi hybrid compartment reported by Ritzenthaler et al. (2002), is not formed or has no time to form and hence AFs are unable to aggregate into clusters.

In contrast to BFA, the phytotropin NPA did not cause any changes in the arrangement of either MTs or AFs (Fig. 3, C, F and I) at concentrations that clearly inhibit NAA transport (Fig. 1A, 2A). The lack of effect on MTs arrangement is consistent with similar observations by Hasenstein et al. (1999) on maize root cells, who found that the inhibition of auxin transport by NPA was not accompanied by changes in the orientation of cortical MTs. Several reports strongly point to an association of the NBP and F-actin filaments (Cox and Muday, 1994; Butler et al., 1998; Hu et al., 2000). Whilst this association seems essential for the inhibitory action of NPA on auxin efflux, the binding of NPA to the NBP appears not to disrupt the association of the NBP with the actin cytoskeleton (Hu et al., 2000; and present results). Thus we conclude that the inhibitory action of NPA on auxin efflux from plant cells is not associated with disruption of the cytoskeletal system.

## **BFA Causes Rapid Changes in mGFP5-ER Distribution**

To follow possible mechanisms underlying the changes in perinuclear actin organization we transformed BY-2 cells with a gene construct coding for an ER-localized GFP variant, mGFP5-ER (Haseloff et al., 1997), containing a C-terminal ER retention signal sequence (HDEL). Using BY-2 cultures expressing this fusion protein, both mobile particles and a static polygonal network of tubules were observed (Fig. 5, A and D) as reported for other fusion proteins containing an HDEL retention signal (Boevink et al., 1996; Haseloff et al., 1997). Since proteins containing HDEL retention sequence might occasionally escape from ER to *cis*-Golgi apparatus, where HDEL binds to a specific receptor (Boevink et al., 1998), the possibility cannot be excluded that the fluorescence signal could be observed also in the structure of *cis*-Golgi. However, it is unlikely that the mobile particles seen in control cells are Golgi stacks because they did not move in the STOP and GO fashion characteristic of Golgi stacks (Nebenführ et al., 1999). One possibility is that they are the small, dilated cisternae of ER described previously in *Brassicaceae* and tobacco guard cells by Hawes et al. (2001). Treatment of cells with 20  $\mu$ M BFA resulted in the appearance of brightly fluorescing static spots at the surface of the ER sheets (Fig 5, B and E). Similar results were reported by Boevink et al. (1999) and Batoko et al. (2000) for the transient expression of a GFP-HDEL-containing protein. These fluorescing spots may be accumulations of GFP in the ER, but a positive identification has not yet been made (C. Hawes, personal communication). The disintegration of the ER that was observed in our experiments is in agreement with results of Henderson et al. (1994), who showed disruption of ER after 3 h treatment with BFA in maize root cells by immunofluorescence microscopy with anti-HDEL antibody. Ritzenthaler et al. (2002) reported that up to 20 min, treatment with BFA causes no visible alteration in ER

morphology in BY-2 cells. Our results indicated that the first observable changes in ER-targeted GFP distribution in BY-2 cells can be seen in as little as 5 minutes after BFA application, when disintegration of the tubular network and formation of fluorescent spots started. In contrast to this NPA did not show any effect on ER-targeted GFP distribution in BY-2 cells. To the best of our knowledge, there are no data about phytohormone effects on ER available yet.

### **The NPA Enigma**

Geldner et al. (2001) reported that TIBA (and possibly also other auxin transport inhibitors) prevented the BFA-induced internalization of PIN1 and the traffic of internalized PIN1 to the PM following the BFA washout. As similar effects of TIBA were observed on the cycling of a PM-ATPase and of the syntaxin KNOLLE, it was suggested that auxin transport inhibitors affect efflux by generally interfering with membrane trafficking processes (Geldner et al., 2001). To generalize from these findings, however, may be premature. Firstly, TIBA does not fulfil the structural requirements of typical phytohormones (Katekar and Geissler, 1980), is a rather weak auxin transport inhibitor, and antagonizes auxin action (Rubery, 1990). Secondly, the concentration of NPA stated to be necessary to bring about a similar reduction in PIN1 cycling (200  $\mu\text{M}$ , Geldner et al., 2001; but no supporting data given) is about two orders of magnitude greater than the concentration of NPA required to saturate inhibition of auxin efflux (1 to 3  $\mu\text{M}$ ; Petrášek et al., 2002, and above). Thirdly, in suspension cultured tobacco cells concentrations of NPA exceeding about 50  $\mu\text{M}$  reduce the stimulation of [ $^3\text{H}$ ]NAA accumulation substantially, possibly as a result of non-specific side effects on the cells unrelated to the specific regulation of auxin efflux (Petrášek et al., 2002, and above). These findings also do not help to explain

why protein synthesis is essential for the inhibitory action of NPA on efflux, but not for the disruption of protein traffic by BFA (Morris et al., 1991; Robinson et al., 1999). There is no information available to address the seemingly crucial question of whether auxin transport inhibitors such as TIBA and NPA affect PIN1 traffic in cells not treated with BFA.

## **CONCLUSIONS**

In this report, measurement of auxin accumulation and observations on the arrangement of the cytoskeleton and ER were performed concurrently on the same population of BY-2 tobacco cells; this enabled us directly to compare the responses of cells at the same stage of development to the phytohormone, NPA, and the vesicle trafficking inhibitor, BFA. Whilst auxin accumulation was stimulated by both NPA or BFA treatments, in contrast to BFA, NPA had no observable effects on the arrangements of MTs, AFs and ER during a 30-min treatment (summarized in Table I). Therefore, although BFA mimics some physiological effects of phytohormones, we conclude from our results that phytohormone effects do not include changes in the arrangement of the cytoskeleton and ER. Furthermore, we find no evidence that conflicts with the view that phytohormones such as NPA inhibit auxin efflux by specific effects on the efflux carrier machinery, rather than by general effects on vesicle traffic.

## **MATERIAL AND METHODS**

### **Plant Material**

BY-2 tobacco cells (*Nicotiana tabacum* L., cv. Bright Yellow 2; Nagata et al., 1992) were cultivated in darkness at 26°C on an orbital incubator (IKA KS501, IKA

Labortechnik, Germany; 120 rpm, orbital diameter 30 mm) in liquid medium (3% w/v sucrose, 4.3 g L<sup>-1</sup> Murashige and Skoog salts, 100 mg L<sup>-1</sup> inositol, 1 mg L<sup>-1</sup> thiamin, 0.2 mg L<sup>-1</sup> 2,4-dichlorophenoxyacetic acid, 200 mg L<sup>-1</sup> KH<sub>2</sub>PO<sub>4</sub>, pH 5.8) and subcultured weekly. Stock BY-2 calli were maintained on media solidified with 0.6% w/v agar and subcultured monthly. Transgenic cells and calli were maintained on the same media supplemented with 100 µg mL<sup>-1</sup> kanamycin and 100 µg mL<sup>-1</sup> cefotaxim. All chemicals were obtained from Sigma unless otherwise stated.

### **Transformation of BY-2 Cells**

The basic transformation protocol of An et al. (1985) was used. A 2-mL aliquot of 3-day old BY-2 cells was co-incubated 3 days with 100 µL of an overnight culture of *Agrobacterium tumefaciens* strain C58C1 carrying pBIN m-*gfp5*-ER plant binary vector (gift of Dr. J. Haseloff, University of Cambridge, UK). It codes for ER-localized GFP variant mGFP5-ER, a thermotolerant derivative of mGFP4-ER (Haseloff et al., 1997), and contains a C-terminal ER retention signal sequence (HDEL). Incubated cells were then washed three times in 50 mL of liquid medium containing 100 µg mL<sup>-1</sup> cefotaxim and plated onto solid medium containing 100 µg mL<sup>-1</sup> kanamycin and 100 µg mL<sup>-1</sup> cefotaxim. Kanamycin-resistant colonies appeared after 3 to 4 weeks of incubation in darkness at 27°C. Cell suspension cultures established from these were maintained as described above, with the addition of 100 µg mL<sup>-1</sup> kanamycin and 100 µg mL<sup>-1</sup> cefotaxim to the cultivation medium.

### **Effects of NPA and BFA on Cytoskeleton Arrangement**

Appropriate volumes of a 25 mM stock solution of BFA in 96% ethanol were added to cell cultures to give final concentrations of 20 µM, 40 µM and 100 µM. NPA

(synthesized in the Institute of Experimental Botany, Prague; cf. Petrášek et al., 2002) was added to cell cultures from 5 mM stock solution in 96% ethanol to a final concentration of 50  $\mu$ M (determined by reference to NPA concentration studies – see above). Equivalent volumes of 96% ethanol were added to all control cultures.

Cell cultures were treated with BFA or NPA for 30 min with continuous shaking at room temperature (approximately 25°C) before microscopic examination (see below). Where required, wash out of BFA was performed with fresh cultivation medium. Aliquots of 10 mL of cell suspension were washed three times (10 min each time) in 50 mL of fresh cultivation medium and filtered on 50-mm diameter cellulose filter paper disks on a Nalgene filter holder. Washed cells were examined immediately.

### **Visualization of Actin Filaments**

AFs were visualized by the method of Kakimoto and Shibaoka (1987) modified according to Olyslaegers and Verbelen (1998). Filtered cells were fixed for 10 min in 1.8% w/v paraformaldehyde (PFA) in standard buffer (PIPES, 50 mM, pH 7.0, supplemented with  $MgCl_2$ , 5 mM, and EGTA, 10 mM). After a subsequent 10-min fixation in standard buffer containing glycerol (1% v/v), cells were rinsed twice for 10 min with standard buffer. Then 0.5 mL of the resuspended cells were incubated for 35 min with the same volume of 0.66  $\mu$ M TRITC-phalloidin prepared freshly from 6.6  $\mu$ M stock solution in 96% ethanol by dilution 1:10 in phosphate buffered saline (PBS; 0.15 M NaCl, 2.7 mM KCl, 1.2 mM  $KH_2PO_4$ , 6.5 mM  $Na_2HPO_4$ , pH 7.2). Cells were then washed three times for 10 min in PBS and observed immediately.

## **Visualization of Microtubules**

MTs were visualized as described in Wick et al. (1981) with the modifications described by Mizuno (1992). After 30 min pre-fixation in 3.7% PFA in microtubule stabilizing buffer consisting of 50 mM PIPES, 2 mM EGTA, 2 mM MgSO<sub>4</sub>, pH 6.9, at 25°C the cells were subsequently fixed in 3.7% PFA and 1% Triton X-100 in microtubule stabilizing buffer for 20 minutes. After treatment with an enzyme solution (1% macerozyme and 0.2% pectinase) for 7 min at 25°C, the cells were attached to poly-L-lysine coated coverslips and treated with 1% Triton X-100 in microtubule stabilizing buffer for 20 minutes. Subsequently, the cells were treated with 0.5% bovine serum albumin in PBS and incubated with a monoclonal mouse antibody against  $\alpha$ -tubulin (DM 1A, Sigma) for 45 minutes at 25°C (dilution 1:500 in PBS). After washing with PBS, a secondary FITC-conjugated anti-mouse antibody (Sigma) diluted 1:80 in PBS was applied for 1 h at 25°C. Coverslips with cells were carefully washed in PBS, rinsed with water and embedded in Mowiol (Polysciences) solution.

## **Microscopy and Image Analysis**

Both fixed and live preparations were observed with an epifluorescence microscope (Nikon Eclipse E600) equipped with appropriate filter sets for FITC and TRITC fluorescence detection. mGFP5-ER fluorescence was observed using the FITC filter set. Pictures and time-lapse scans were grabbed with a monochrome integrating CCD camera (COHU 4910, USA) and digitally stored.

LUCIA image analysis software (Laboratory Imaging, Prague, Czech Republic) was used for the evaluation of the effect of BFA on perinuclear actin aggregation. Pictures of TRITC-phalloidin-stained AFs were transformed to

complementary colors (Fig. 3, A and C) and a measuring mask was applied interactively over the perinuclear region (Fig. 3, B and D). The density variation (DV) parameter was measured. The DV parameter is the standard deviation of optical density values under the measuring mask, where the bigger the DV, the higher the aggregation of actin. Approximately 300 cells in ten optical fields were assessed for each sample.

### **Auxin Accumulation Measurement**

Auxin accumulation by cells was measured according to the method of Delbarre et al. (1996), modified by Petrášek et al. (2002). The accumulation by the cells of [<sup>3</sup>H]NAA (specific radioactivity 935 GBq x mmol<sup>-1</sup>, synthesized at the Isotope Laboratory, Institute of Experimental Botany, Prague, Czech Republic), was measured in 0.5 mL aliquots of cell suspension (cell density ca. 7 x 10<sup>5</sup> cells mL<sup>-1</sup>, as determined by counting cells in Fuchs-Rosenthal haemocytometer). Each cell suspension was filtered, re-suspended in uptake buffer (20 mM MES, 40 mM sucrose, 0.5 mM CaSO<sub>4</sub>, pH adjusted to 5.7 with KOH) and equilibrated for 45 min with continuous orbital shaking. Equilibrated cells were collected by filtration, re-suspended in fresh uptake buffer and incubated on the orbital shaker for 1.5 h in darkness at 25°C. [<sup>3</sup>H]NAA was added to the cell suspension to give a final concentration of 2 nM. After a timed uptake period (depending on experiment, see above) 0.5 mL aliquots of suspension were withdrawn and accumulation of label was terminated by rapid filtration under reduced pressure on 22 mm diameter cellulose filters. The cell cakes and filters were transferred to scintillation vials, extracted in ethanol for 30 min and radioactivity was determined by liquid scintillation counting (Packard Tri-Carb 2900TR scintillation counter). Counts were corrected for surface radioactivity by

subtracting counts obtained for aliquots of cells collected immediately after the addition of [<sup>3</sup>H]NAA. Counting efficiency was determined by automatic external standardization, and counts were corrected automatically. NPA or BFA were added as required from ethanolic stock solutions to give the appropriate final concentration (see above). In time-course experiments, aliquots of cell suspension were removed at timed intervals varying from 0 to 40 minutes from the start of experiments; the concentration-dependence of auxin accumulation in response to NPA or BFA was determined after a 20-min uptake period.

### **Metabolism of Labeled Compounds**

Possible distortion of the results of auxin accumulation studies by metabolism of the [<sup>3</sup>H]NAA taken up by the cells was checked. Cells of BY-2 were incubated for 30 min as described in the presence of 2 nM [<sup>3</sup>H]NAA. At the end of the incubation period, 10-mL aliquots of the incubated suspensions were quickly filtered on paper with gentle suction, washed rapidly with 5 mL of uptake buffer, and the cell cake was transferred to 2 mL pre-chilled ethanol and stored at -80 °C until required. Cell debris was removed by filtration under gentle pressure through cellulose filters. Radioactive compounds in the extracts were separated by chromatography on cellulose thin layer plates (POLYGRAM CEL 300 UV<sub>254</sub>, Macherey-Nagel, Düren, Germany), together with samples of the labeled auxins. The plates were developed in three independent solvent systems: (a) *isopropanol*:26% (v/v) ammonia:water (10:1:1, v/v/v); (b) chloroform:ethanol:glacial acetic acid (95:1:5, v/v/v); and (c) chloroform:ethanol:glacial acetic acid (75:20:5, v/v/v). Each chromatogram strip was cut into 20 sequential segments, eluted in ethanol and counted by liquid scintillation counting.

## **ACKNOWLEDGEMENTS**

Authors thank Dr. Jim Haseloff (University of Cambridge, UK) for the pBIN m-*gfp5*-ER binary vector, and Miss Andrea Hourová for her excellent technical assistance.

## LITERATURE CITED

- Alvarez C, Sztul ES (1999) Brefeldin A (BFA) disrupts the organization of the microtubule and the actin cytoskeletons. *Eur J Cell Biol* 78: 1-14
- An G (1985) High efficiency transformation of cultured tobacco cells. *Plant Physiol* 79: 568-570
- Bernasconi P, Patel BC, Reagan JD, Subramanian MV (1996) The N-1-naphthylphthalamic acid-binding protein is an integral membrane protein. *Plant Physiol* 111: 427-432
- Batoko H, Zheng HQ, Hawes C, Moore I (2000) A Rab1 GTPase is required for transport between the endoplasmic reticulum and Golgi apparatus and for normal Golgi movement in plants. *Plant Cell* 12: 2201-2217
- Boevink P, Santa Cruz S, Hawes C, Harris N, Oparka KJ (1996) Virus-mediated delivery of the green fluorescent protein to the endoplasmic reticulum of plant cells. *Plant J* 10: 935-941
- Boevink P, Oparka K., Santa Cruz S, Martin B, Betteridge A, Hawes C (1998) Stacks on tracks: the plant Golgi apparatus traffics on an actin/ER network. *Plant J* 15: 441-447
- Boevink P, Martin B, Oparka K, Santa Cruz S, Hawes C (1999) Transport of virally expressed green fluorescent protein through the secretory pathway in tobacco leaves is inhibited by cold shock and brefeldin A. *Planta* 208: 392-400
- Butler JH, Hu SQ, Brady SR, Dixon MW, Muday GK (1998) In vitro and in vivo evidence for actin association of the naphthylphthalamic acid-binding protein from zucchini hypocotyls. *Plant J* 13: 291-301

- Cande WZ, Goldsmith MHM, Ray PM (1973) Polar auxin transport and auxin-induced elongation in the absence of cytoplasmic streaming. *Planta* 111: 279-296
- Cox DN, Muday GK (1994) NPA binding activity is peripheral to the plasma membrane and is associated with the cytoskeleton. *Plant Cell* 6: 1941-1953
- Davies PJ (1995) The plant hormone concept: Concentration, sensitivity and transport. In PJ Davies, ed, *Plant Hormones: Physiology, Biochemistry and Molecular Biology*, 2nd edn. Dordrecht, Boston, London: Kluwer Academic Publishers, pp 13-38
- Delbarre A, Muller P, Imhoff V, Guern J (1996) Comparison of mechanisms controlling uptake and accumulation of 2,4-dichlorophenoxy acetic acid, naphthalene-1-acetic acid, and indole 3-acetic acid in suspension-cultured tobacco cells. *Planta* 198: 532-541
- Delbarre A, Muller P, Guern J (1998) Short-lived and phosphorylated proteins contribute to carrier-mediated efflux, but not to influx, of auxin in suspension-cultured tobacco cells. *Plant Physiol* 116: 833-844
- Dixon MW, Jacobson JA, Cady CT, Muday GK (1996) Cytoplasmic orientation of the naphthylphthalamic acid-binding protein in zucchini plasma membrane vesicles. *Plant Physiol* 112: 421-432
- Friml J, Palme K (2002) Polar auxin transport - old questions and new concepts? *Plant Mol Biol* 49: 273-284
- Gälweiler L, Guan C, Müller A, Wisman E, Mendgen K, Yephremov A, Palme K (1998) Regulation of polar auxin transport by AtPIN1 in *Arabidopsis* vascular tissue. *Science* 282: 2226-2230

- Geldner N, Friml J, Stierhof YD, Jürgens G, Palme K (2001) Auxin transport inhibitors block PIN 1 cycling and vesicle trafficking. *Nature* 413: 425-428
- Goldsmith MHM (1977) The polar transport of auxin. *Annu Rev Plant Physiol* 28: 439-478
- Haseloff J, Siemering KR, Prasher DC, Hodge S (1997) Removal of a cryptic intron and subcellular localisation of green fluorescent protein are required to mark transgenic *Arabidopsis* plants brightly. *Proc Natl Acad Sci USA* 94: 2122-2127
- Hasenstein KH, Blancaflor EB, Lee JS (1999) The microtubule cytoskeleton does not integrate auxin transport and gravitropism in maize roots. *Physiol Plant* 105: 729-738
- Hawes C, Saint-Jore C, Martin B, Zheng HQ (2001) ER confirmed as the location of mystery organelles in *Arabidopsis* plants expressing GFP! *Trends Plant Sci* 6: 245-246
- Henderson J, Satiat-Jeunemaitre B, Napier R, Hawes C (1994) Brefeldin A-induced disassembly of the Golgi apparatus is followed by disruption of the endoplasmic reticulum in plant cells. *J Exp Bot* 45: 1347-1351
- Hu SQ, Brady SR, Kovar DR, Staiger CJ, Clark GB, Roux SJ, Muday GK (2000) Identification of plant actin binding proteins by F-actin affinity chromatography. *Plant J* 24: 127-137
- Kakimoto T, Shibaoka H (1987) Actin filaments and microtubules in the preprophase band and phragmoplast of tobacco cells. *Protoplasma* 140: 151-156
- Katekar GF, Geissler AE (1980) Auxin transport inhibitors: IV. Evidence of a common mode of action for a proposed class of auxin transport inhibitors: The phytotropins. *Plant Physiol* 66: 1190-1195

- Kumagai F, Hasezawa S (2001) Dynamic organization of microtubules and microfilaments during cell cycle progression in higher plant cells. *Plant Biology* 3: 4-16
- Lomax TL, Muday GK and Rubery PH (1995) Auxin transport. In: Davies PJ (ed) *Plant Hormones: Physiology, Biochemistry and Molecular Biology*, 2nd edn. Dordrecht, Boston, London: Kluwer Academic Publishers, pp 509-530
- Mizuno K (1992) Induction of cold stability of microtubules in cultured tobacco cells. *Plant Physiol* 100: 740-748
- Morris DA (2000) Transmembrane auxin carrier systems - dynamic regulators of polar auxin transport. *Plant Growth Regul* 32: 161-172
- Morris DA, Rubery PH, Jarman J, Sabater M (1991) Effects of inhibitors of protein synthesis on transmembrane auxin transport in *Cucurbita-pepo* L. hypocotyl segments. *J Exp Bot* 42: 773-783
- Morris DA, Robinson JS (1998) Targeting of auxin carriers to the plasma membrane: differential effects of brefeldin A on the traffic of auxin uptake and efflux carriers. *Planta* 205: 606-612
- Müller A, Guan CH, Gälweiler L, Tänzler P, Huijser P, Marchant, A, Parry G, Bennett M, Wisman E, Palme K (1998) *AtPIN2* defines a locus of *Arabidopsis* for root gravitropism control. *EMBO J* 17: 6903-6911
- Muday GK (2000) Maintenance of asymmetric cellular localization of an auxin transport protein through interaction with the actin cytoskeleton. *J Plant Growth Regul* 19: 385-396
- Muday GK, DeLong A (2001) Polar auxin transport: controlling where and how much. *Trends Plant Sci* 6: 535-542

- Muday GK, Murphy AS (2002) An emerging model of auxin transport regulation. *Plant Cell* 14: 293-299
- Nagata T, Nemoto Y, Hasezawa S (1992) Tobacco BY-2 cell line as the “Hela” cell in the cell biology of higher plants. *Int. Rev. Cytol.* 132: 1-30
- Nebenführ A, Gallagher LA, Dunahay TG, Frohlick JA, Mazurkiewicz AM, Meehl JB, Staehelin LA (1999) Stop-and-go movements of plant Golgi stacks are mediated by the acto-myosin system. *Plant Physiol* 121: 1127-1141
- Nebenführ A, Staehelin LA (2001) Mobile factories: Golgi dynamics in plant cells. *Trends Plant Sci* 4: 160-167
- Olyslaegers G, Verbelen JP (1998) Improved staining of F-actin and co-localization of mitochondria in plant cells. *J Microsc-Oxford* 192: 73-77
- Petrášek J, Elčknér M, Morris DA, Zažímalová E (2002) Auxin efflux carrier activity and auxin accumulation regulate cell division and polarity in tobacco cells. *Planta*, *in press* (DOI 10.1007/s00425-002-0845-y)
- Raven JA (1975) Transport of indoleacetic acid in plant cells in relation to pH and electrical potential gradients, and its significance for polar IAA transport. *New Phytol* 74: 163-174
- Ritzenthaler C, Nebenführ A, Movafeghi A, Stussi-Garaud C, Behnia L, Pimpl P, Staehelin LA, Robinson DG (2002) Reevaluation of the effects of brefeldin A on plant cells using tobacco bright yellow 2 cells expressing Golgi-targeted green fluorescent protein and COPI antisera. *Plant Cell* 14: 237-261

- Robinson JS, Albert AC, Morris DA (1999) Differential effects of brefeldin A and cycloheximide on the activity of auxin efflux in *Cucurbita pepo* L. *J. Plant Physiol* 155: 678-684
- Rubery PH (1990) Phytotropins: receptors and endogenous ligands. *Symp. Soc. Exp. Biol.* 44: 119-146
- Rubery PH, Sheldrake AR (1974) Carrier-mediated auxin transport. *Planta* 188: 101-121
- Satiat-Jeunemaitre B, Steele C, Hawes C (1996) Golgi-membrane dynamics are cytoskeleton dependent: A study on Golgi stack movement induced by brefeldin A. *Protoplasma* 191: 21-33
- Saint-Jore CM, Evins J, Batoko H, Brandizzi F, Moore I, Hawes C (2002) Redistribution of membrane proteins between the Golgi apparatus and endoplasmic reticulum in plants is reversible and not dependent on cytoskeletal networks. *Plant J* 29: 661-678
- Sussman MR, Gardner G (1980) Solubilization of the receptor for N-1-naphthylphthalamic acid. *Plant Physiol* 66: 1074-1078
- Swarup R, Friml J, Marchant A, Ljung K, Sandberg G, Palme K, Bennett M (2001) Localization of the auxin permease AUX1 suggests two functionally distinct hormone transport pathways operate in the *Arabidopsis* root apex. *Gene Dev* 15: 2648-2653
- Waller F, Riemann M, Nick P (2002) A role of actin-driven secretion in auxin-induced growth. *Protoplasma* 219: 72-81

Wick SM, Seagull RW, Osborn M, Weber K and Gunning BES (1981)

Immunofluorescence microscopy of organized microtubule arrays in structurally stabilized meristematic plant cells. *J. Cell Biol* 89 (3): 685-690

Wilkinson S, Morris DA (1994) Targeting of auxin carriers to the plasma membrane: effects of monensin on transmembrane auxin transport in *Cucurbita pepo* L. tissue. *Planta* 193: 194-202

## FIGURE CAPTIONS

**Figure 1.** The effect of 1-*N*-naphthylphthalamic acid (NPA) and brefeldin A (BFA) on the accumulation of [<sup>3</sup>H]-naphthalene-1-acetic acid ([<sup>3</sup>H]NAA) in 2-day old BY-2 cells. **A** [<sup>3</sup>H]NAA accumulation in the absence (●, control) and in the presence of 10 μM (○), 50 μM (■) and 200 μM (□) NPA. **B** [<sup>3</sup>H]NAA accumulation in the absence (●, control) and in the presence of 20 μM (○), 40 μM (■) and 100 μM (□) BFA. Error bars represent SEs of the mean (n = 3).

**Figure 2.** The effect of concentration of 1-*N*-naphthylphthalamic acid (NPA) (**A**) and brefeldin A (BFA) (**B**) on the accumulation of [<sup>3</sup>H]-naphthalene-1-acetic acid ([<sup>3</sup>H]NAA) by 2-day old BY-2 cells. Error bars represent SEs of the mean (n = 4).

**Figure 3.** The effect of brefeldin A (BFA) and 1-*N*-naphthylphthalamic acid (NPA) on the arrangement of actin filaments (AFs) and microtubules (MTs) in 2-day old BY-2 cells. **A, D, G** Control cells with fine AFs in cortical region (**A**); radially oriented AFs in transvacuolar strands (**D**); and transversely oriented cortical MTs (**G**). **B, E, H** AFs and cortical MTs after 30 min incubation in 20 μM BFA. Modification of AFs staining pattern in cortical (**B**) and perinuclear region (**E**), where AFs in transvacuolar strands are "pulled down" forming clusters around the nucleus. **H** Unaffected arrangement of cortical MTs. **C, F, I** AFs and cortical MTs after 30 min incubation in 50 μM NPA. Unaltered AFs staining pattern in the cortical (**C**) and perinuclear region (**F**). **I** Transversally oriented cortical MTs with no obvious changes. Scale bars = 10 μm.

**Figure 4.** The quantification of brefeldin A (BFA) effect on actin filaments (AFs). **A, C** Grabbed images of TRITC-phalloidin-stained control (**A**) and BFA-treated cells (**C**) after transformation to complement colors. **B, D** Interactively applied measuring mask over the perinuclear region for the measurement of the relative optical density variation (DV) parameter. See Material and Methods for details. **E** Relative optical DV in control (empty columns) and in the presence of 20  $\mu\text{M}$  (shaded columns), 40  $\mu\text{M}$  (checked columns) and 100  $\mu\text{M}$  (full columns) BFA. **F** Relative optical DV in wash out experiment. BFA (20  $\mu\text{M}$ , shaded columns) was washed out with fresh medium and optical DV scored after 30-min incubation (empty column). Error bars represents SEs of the mean (n=10, 300 cells in total).

**Figure 5.** The effect of brefeldin A (BFA) and 1-*N*-naphthylphthalamic acid (NPA) on the arrangement of endoplasmic reticulum (ER) in 2-day old BY-2 cells expressing mGFP5-ER. **A, D** GFP fluorescence in control cells. Optical cuts through cortical region (**A**) and perinuclear region (**D**). **B, E** GFP fluorescence in cells after 30-min incubation in 20  $\mu\text{M}$  BFA. The formation of bright fluorescence spots (**B**) and large sheets (**B**, asterisks) in the cortical layer are shown. Bright fluorescence spots in transvacuolar strands and in the perinuclear region (**E**). Video files showing control cells and the effect 30-min incubation in 20  $\mu\text{M}$  BFA can be seen at:

[http://www.ueb.cas.cz/laboratory\\_of\\_hormonal\\_regulations/BFAmovies.htm](http://www.ueb.cas.cz/laboratory_of_hormonal_regulations/BFAmovies.htm)

**C, F** GFP fluorescence in cells after 30-min incubation in 50  $\mu\text{M}$  NPA. Unaltered ER in the cortical (**C**) and perinuclear region (**F**). Bars 10  $\mu\text{m}$ .

**Table I.** Summary of the effects of NPA (10-200  $\mu$ M) and BFA (20-100  $\mu$ M) on cell structures and auxin accumulation in suspension-cultured 2-day old BY-2 tobacco cells

	Microtubules	Actin filaments	Endoplasmic reticulum	Auxin accumulation
1-N-naphthylphthalamic acid (NPA)	–	–	–	+
brefeldin A (BFA)	–	+	+	+

– No differences from control observed. + Structure affected, auxin accumulation increased.

Fig. 1

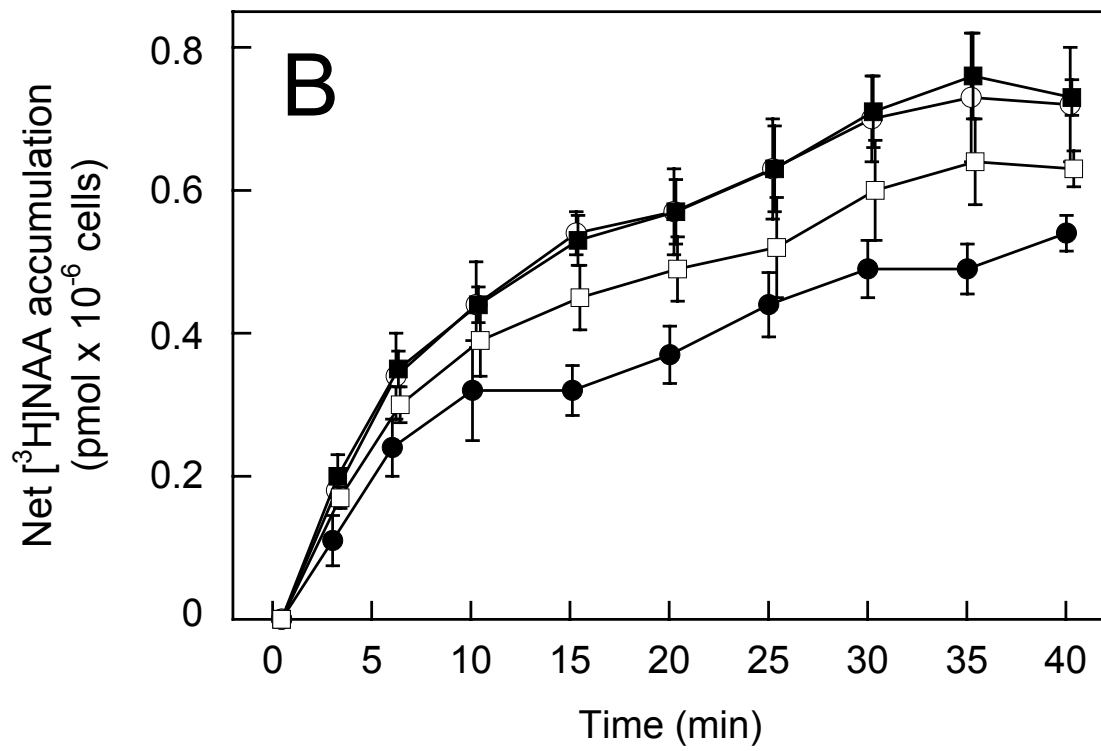
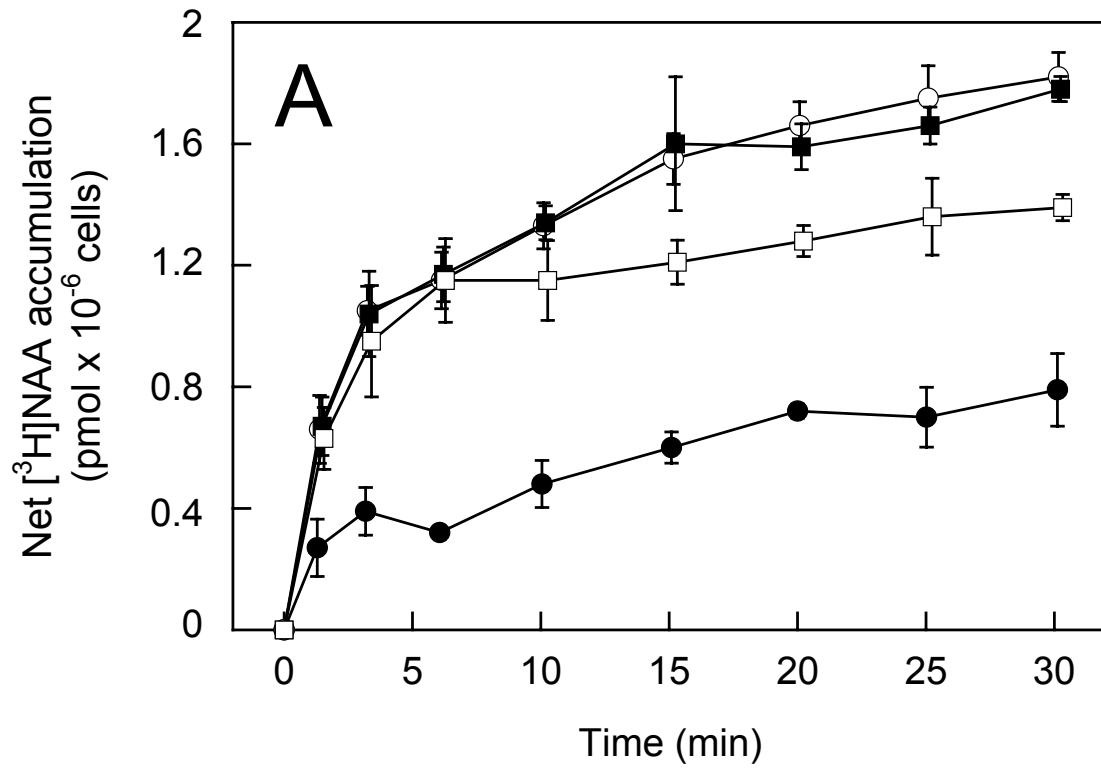


Fig. 2

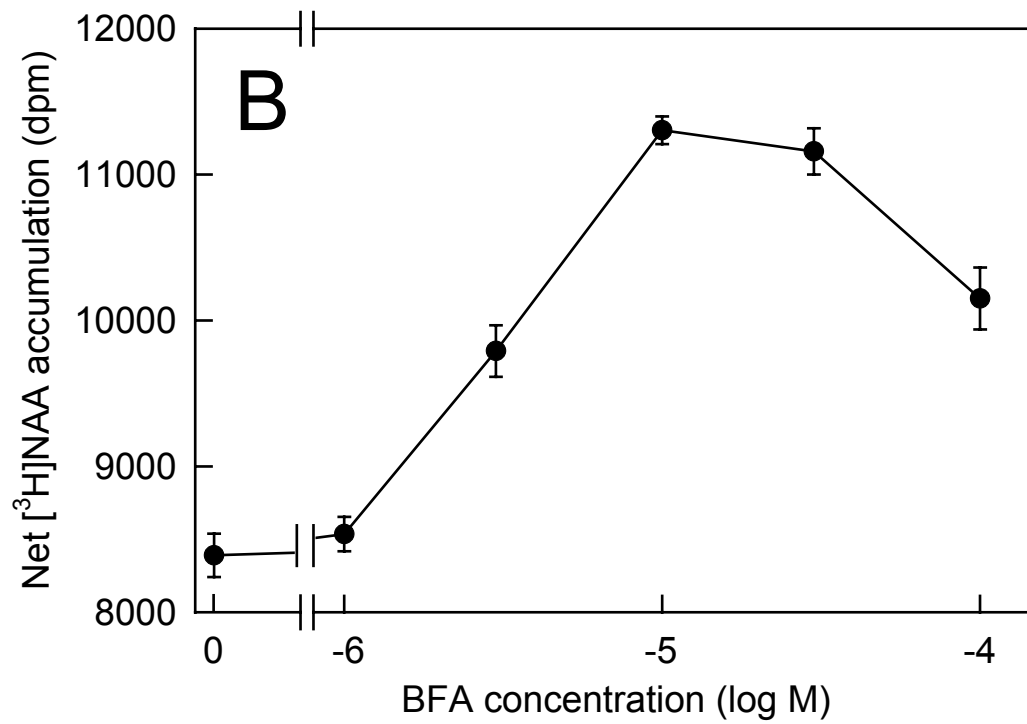
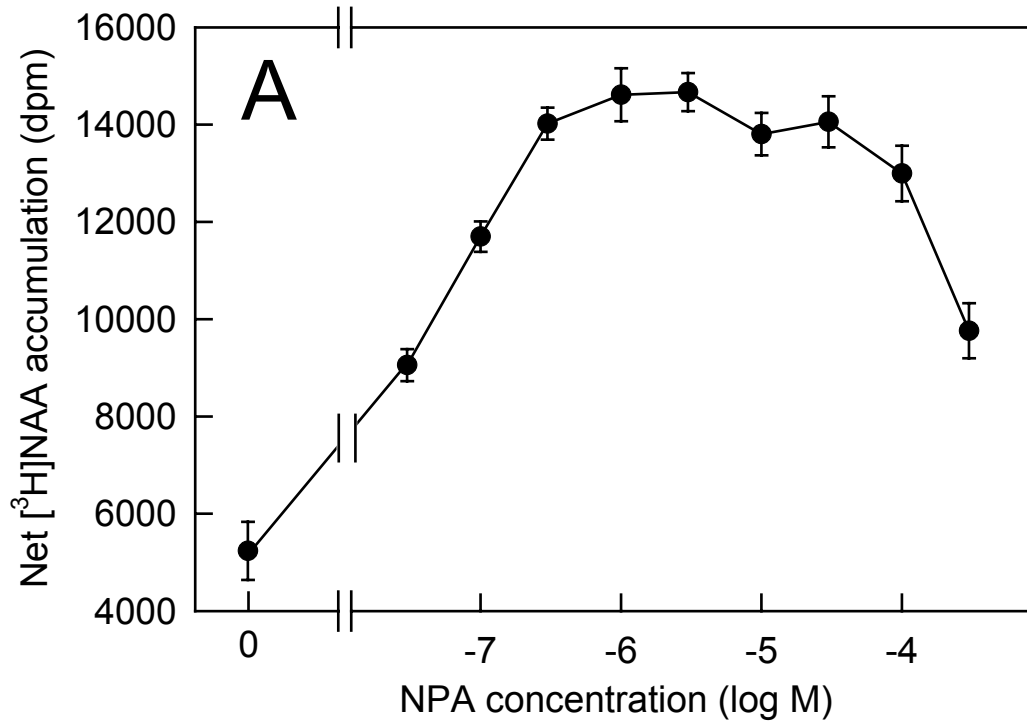


Fig. 3

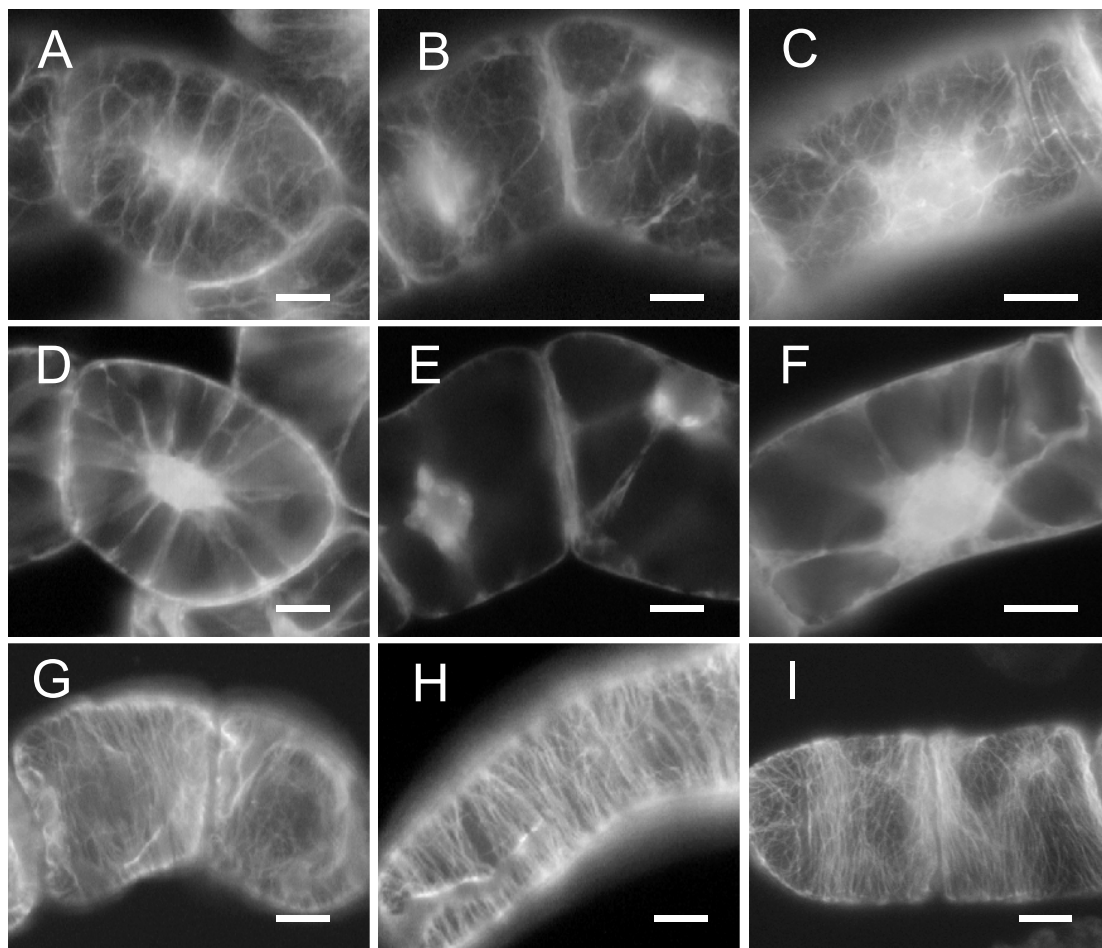


Fig. 4

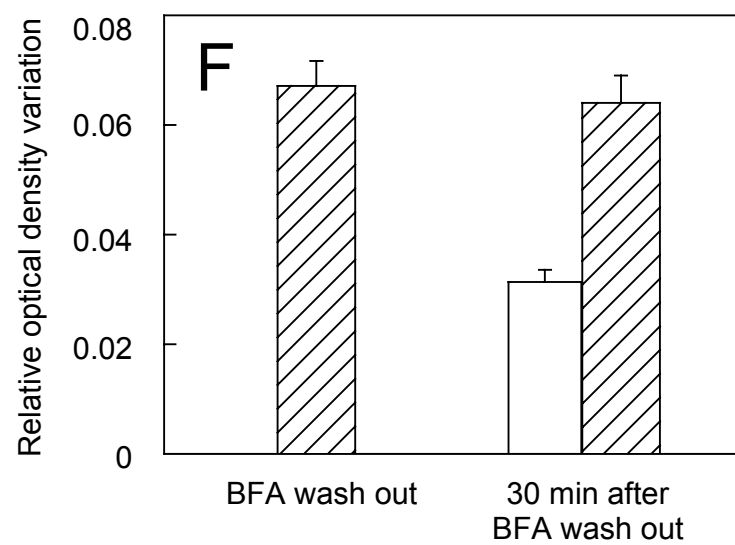
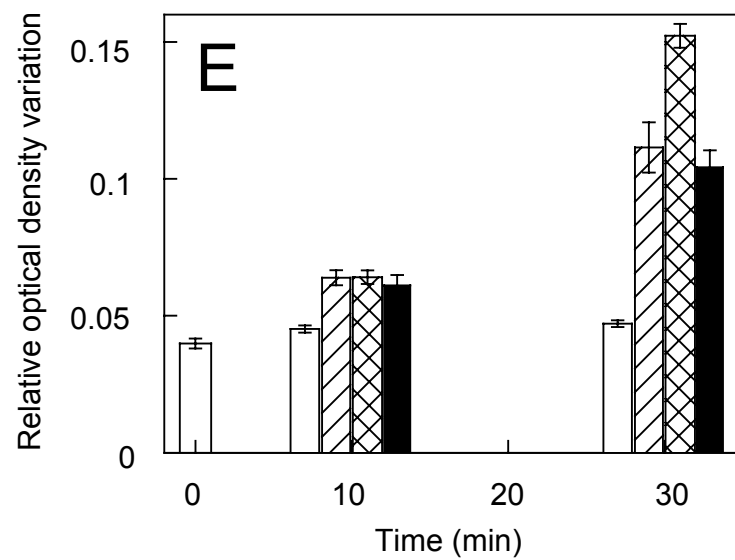
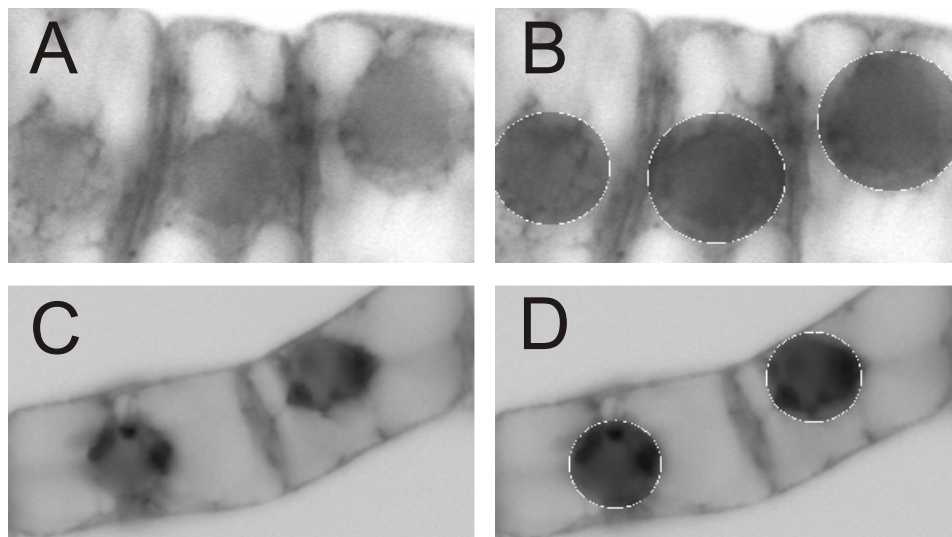


Fig. 5

